

## ON THE EVOLUTION OF ULTRACOMPACT H II REGIONS

ERIC KETO

Harvard-Smithsonian Center for Astrophysics, 60 Garden Street, Cambridge, MA 02138

Received 2002 April 23; accepted 2002 July 30

### ABSTRACT

The classic model for the pressure-driven expansion of H II regions is reevaluated to include the gravitational force of the star responsible for the H II region. The model shows that the gravitational attraction of the star maintains a steep density gradient and accretion flow within the ionized gas and prevents the H II region from expanding hydrodynamically unless the radius of ionization equilibrium is beyond the radius where the sound speed of the ionized gas approximates the escape velocity. Once past this critical radius, the H II region will expand rapidly and the accretion flow through the H II region is quickly reduced. However, in contrast to the model without gravity in which the velocity of the ionized gas is everywhere outward, in the model with gravity, the velocity within the H II region is always inward. Newly formed massive stars within dense molecular cores may initially form very small H II regions that at first evolve slowly through an increase in ionizing flux, as would be caused by an increase in the mass or number of stars through continuing accretion through the H II region.

*Subject headings:* accretion, accretion disks — H II regions — hydrodynamics

### 1. INTRODUCTION

In the classic model for the pressure-driven evolution of H II regions, an H II region is first formed when a newly born massive star begins to ionize a surrounding cloud that is assumed to be static, uniform in density, and of infinite extent. Initially, the ionization front moves rapidly through the cloud until equilibrium is obtained between the flux of ionizing photons from the star and the number of recombinations within the H II region. The density within this new H II region is approximately the same as the surrounding gas, but the temperature is about 100 times higher. The higher pressure causes the H II region to expand and drives a shock into the surrounding neutral gas. As the expansion reduces the density of the ionized gas and therefore the recombination rate, more ionizing photons reach the ionization front, which continues to move outward to reestablish equilibrium. Descriptions can be found in standard textbooks such as Spitzer (1978), Dyson & Williams (1980), and Shu (1992). This classic model for pressure-driven expansion has also been extended by Franco, Tenorio-Tagle, & Bodenheimer (1990) to describe the evolution of H II regions within clouds that have power-law density gradients.

This model is simple, compelling, and has been widely used to interpret observations of H II regions of all sizes in many different environments (Mathews & O'Dell 1969; Yorke 1986; Garay & Lizano 1999). Because of the assumption that the gravitational attraction of the star is negligible compared to the gas pressure ( $GM^2/rnkT \ll 1$ ), the model is most appropriate in describing the evolution of older, giant optical H II regions, whose ionization and shock fronts are at sufficiently large radii that the stellar gravitational field is negligible. The model is least successful in describing the evolution of small ultracompact H II (UCH II) regions of massive star-forming regions where the stellar gravitational attraction can be significant at small scales.

This paper shows how the effect of the gravitational attraction of the ionizing star may be included in the model for pressure-driven expansion to produce a description of the evolution of H II regions more appropriate for the condi-

tions immediately following star formation. In this model, when a massive protostar begins nuclear burning in a dense molecular core, the H II region forms within the steep density gradient and accretion flow caused by the star's gravitational field. The evolution of the H II region within this molecular accretion flow is described by the same assumptions and equations as in the original model for pressure-driven expansion: spherical symmetry, constant flow, conservation of mass, isothermal equation of state, photoionization equilibrium, and the jump conditions across the ionization and shock fronts at the H II region boundary, but now including the gravitational attraction of the star while still ignoring the self-gravity of the gas. With this set of equations, the accretion flow is described by Bernoulli's equation (Bondi 1952). This paper shows how the evolution of the H II region and the accretion flow can be solved self-consistently in a manner similar to that used to derive the evolutionary solution for the classic model without gravity but the resulting evolution is significantly different.

The evolutionary solution shows that in the earliest stages at small radii, the thermal pressure differential is small compared to the gravitational force, and the H II region cannot expand by thermal pressure. Pressure-driven expansion can only occur if the boundary of the H II region is beyond a radius where the sound speed of the ionized gas exceeds the escape velocity of the stellar gravitational attraction. More precisely, this radius is where the ionization front makes a transition from R-critical to D-critical just before the sonic point of the ionized accretion flow. If a smaller H II region is to expand up to this point, then it must be by increasing the ionizing flux from the stars, perhaps by stellar evolution or by an increase in the mass or number of stars through ongoing accretion. However, once the boundary is past this critical point, the thermal expansion can begin. The expansion reduces the inward velocities in the H II region and rarefies the ionized gas with the result that the mass accretion rate through the H II region is diminished almost to zero. Outside the boundary shock, because the gas is not affected by the disturbances arising from the boundary, the neutral accretion flow toward the H II boundary continues

unchanged, with the result that the neutral gas piles up in the boundary layer between the ionization and shock fronts.

The solution shows that at all evolutionary stages, the neutral accretion flow continues to pass through the boundary of the H II region and continues inward toward the star as an ionized accretion flow despite the expansion of the H II region. The direction of flow within the H II region is a significant difference between the two evolutionary models. In the classic model without gravity, the velocity of the ionized gas is always outward with the highest velocity just inside the boundary of the H II region. With gravity, the velocity is always inward with the highest velocities at the center of the H II region. A recent observation indicating inward motion within an H II region can be found in Keto (2002).

## 2. DESCRIPTION OF THE MODEL

A star of mass  $M$  with a flux of ionizing photons  $N_*$  is at the center of a spherically symmetric, steady accretion flow driven by the gravitational attraction of the star. The self-gravity of the gas is ignored. The stellar radiation maintains an ionized region around the star in equilibrium with the recombination rate within the H II region. Both the ionized and neutral zones are assumed to be at constant temperature. Following the treatment in Bondi (1952) and Mestel (1954), the hydrodynamic equations may be written in non-dimensional form using the scaling factors,

$$r = \left( \frac{GM}{c_1^2} \right) x, \quad v = \left( c_1 \frac{K_i}{K_1} \right) y, \quad \rho = \left( \rho_1 \frac{K_1}{K_i} \right) z, \quad (1)$$

where the subscript  $i = 1, 2$  refers to the neutral and ionized zones, and where  $K_1 = RT_1$  and  $K_2 = jRT_2$ , where  $R$  is the gas constant,  $T_i$  is the temperature in zones 1 and 2, and the factor  $j$  is the number of nuclei and electrons resulting from the ionization of an atom or molecule of gas in the neutral zone. For example,  $j = 2$  if the neutral gas is composed purely of atomic hydrogen, and  $j = 4$  if it is molecular hydrogen. The velocity of sound is  $\sqrt{K_i}$  in each zone.

The equation of motion of an isothermal gas in a spherically symmetric gravitational field integrates to Bernoulli's equation,

$$\frac{1}{2}v^2 + \int \frac{dP}{\rho} - \frac{GM}{r} = \text{constant}, \quad (2)$$

while the equation of continuity is

$$\dot{M} = 4\pi r^2 \rho v, \quad (3)$$

where  $\dot{M}$  is the accretion rate. Prior to ionization, the neutral accretion flow will extend from infinity to the stellar surface. With the condition of zero velocity at infinity and using the scaling relations (eq. [1]), these last two equations may be combined as

$$\ln \lambda = \left( \frac{1}{x} + 2 \ln x \right) - \left( \frac{1}{2}y^2 - \ln y \right), \quad (4)$$

where

$$\dot{M} = 4\pi\lambda(GM)^2 c_1^{-3} \rho_\infty. \quad (5)$$

The well-known solutions to equations (4) and (2) are shown in Figures 1 and 2. In Figure 1, the two solutions passing through the sonic point at  $r_s = GM_*/2c_1^2$ ,  $y = c_1$  or

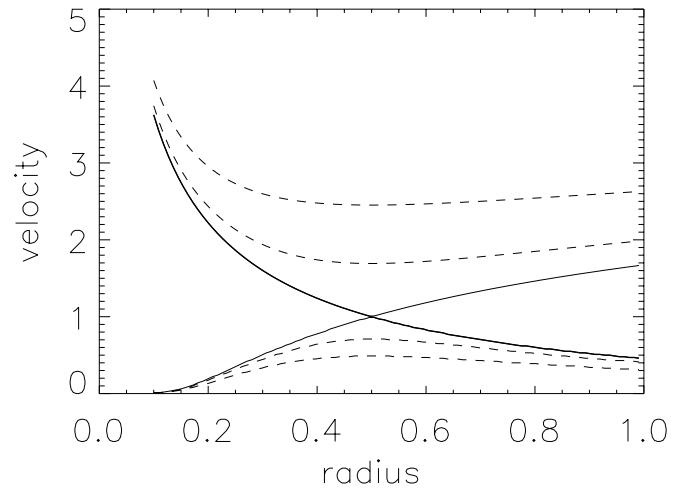


FIG. 1.—Solutions of the Bernoulli equation (eq. [2]). The two solid lines show the solution for the Bondi accretion problem and for the Parker isothermal wind. The accretion solution is supersonic at small radii and subsonic at large radii, and the wind solution is the opposite. Both solutions pass through the sonic point at  $x, y = \frac{1}{2}, 1$ , and these are the only two transonic solutions. The dashed lines show other solutions that are either supersonic or subsonic over the whole range of radii. The units are nondimensional, scaled according to eq. (1).

$x = \frac{1}{2}, y = 1$ , are the solutions for accretion (Bondi 1952) and an isothermal stellar wind (Parker 1958). At the sonic point, both the terms in equation (4),  $(x^{-1} + 2 \ln x)$  and  $(\frac{1}{2}y^2 - \ln y)$ , have minima and  $\ln \lambda = 0.1138$ . This fixed value of  $\lambda$  means that once the stellar mass, the sound speed, and the density at infinity are specified, the accretion rate (eq. [5]) is uniquely determined. Another way to see this restriction is to take the derivative of equation (2) which yields the equation of motion,

$$\frac{1}{y} \frac{dy}{dx} = \left( \frac{1}{x^2} + \frac{2}{x} \right) / (1 - y^2). \quad (6)$$

Any solution in which the flow starts subsonic and transi-

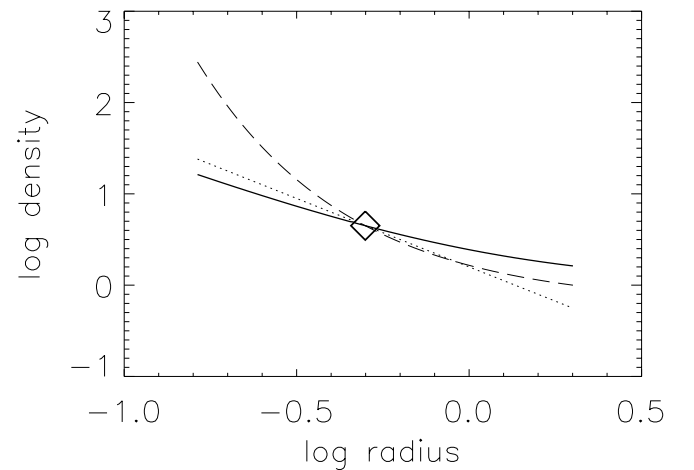


FIG. 2.—Density profile of the trans-sonic accretion solution (solid line) compared with the free-fall profile,  $n \sim r^{-3/2}$  (dotted line), and the density in hydrostatic equilibrium,  $n \sim \exp(2r_s/r)$  (dashed line). The accretion solution approximates free fall at radii below the sonic point (diamond) and approximates hydrostatic equilibrium at larger radii. The units are the log of the nondimensional variables, scaled according to eq. (1).

tions to supersonic must pass through the sonic point,  $x = \frac{1}{2}$ ,  $y = 1$ , to avoid a nonphysical infinite acceleration. Other solutions that are entirely subsonic or supersonic are also possible as shown in Figure 1. However, these solutions would not satisfy the boundary conditions for an accretion flow at both zero and infinity.

Since the equations (2) or (6) involve only the variables  $x$  and  $y$ , the velocity of the flow is completely determined by the mass of the star and the sound speed. Once the velocity profile is set, the conservation equation determines the density profile subject to a scaling factor that is the density at infinity. Figure 2 shows the density profile of the trans-sonic accretion solution in comparison with the density profiles for free fall,  $\rho \sim r^{-3/2}$ , and hydrostatic equilibrium. The accretion solution approximates the free-fall solution at radii less than the sonic point where gravitational forces dominate. At larger radii, the solution approximates hydrostatic equilibrium as pressure forces dominate.

If there is an H II region within the accretion flow, the flow within both the ionized and neutral zones will obey the energy equation (2) and the conservation equation (3) within each zone. The solutions must also match at the interface through the jump conditions,

$$\rho_1 v_1 = \rho_2 v_2, \quad (7)$$

$$\rho_1 (v_1^2 + c_1^2) = \rho_2 (v_2^2 + c_2^2), \quad (8)$$

or in nondimensional form,

$$y_1 z_1 = y_2 z_2, \quad (9)$$

$$z_1 (1 + y_1^2) = z_2 (1 + K_2/K_1 y_1^2). \quad (10)$$

The interface also provides the energy constant for the streamlines of the ionized flow,

$$\left( \frac{1}{2} y_2^2 - \frac{K_1}{K_2} \ln y_2 \right) - \frac{K_1}{K_2} \left( 2 \ln x + \frac{K_1}{K_2} \frac{1}{x} \right) = \text{constant} \equiv \beta, \quad (11)$$

$$\beta = -\frac{K_1}{K_2} \ln \lambda_2 + \frac{1}{2} y_{2f}^2 + \ln z_{2f} - \frac{1}{x_f}, \quad (12)$$

where the additional subscript “ $f$ ” refers to conditions at the ionization front, and  $2f$  refers specifically to the conditions on the ionized side of the front. The mass infall rate in the ionized zone is  $\lambda_2$ . In this model, since the gravitational attraction at small radii dominates the thermal pressure differential, the gas continues to fall toward the star and is assumed to disappear into the star at the stellar radius without specifying further the effect on the star.

The position of the interface,  $x$ , is set by ionization equilibrium within the H II region. Since the accretion rate is constant, the mass within the H II region is constant if the ionization front is stationary. The radius of ionization equilibrium,  $r_f$ , is set by the balance of ionizations, equal to the rate of ionizing photons,  $J_*$ , from the star, and the rate of recombinations within the H II region,

$$J_* = \int_{r_*}^{r_f} \alpha n_e^2 4\pi r' dr', \quad (13)$$

where  $\alpha$  is the recombination coefficient, about  $3 \times 10^{-13} \text{ cm}^3 \text{ s}^{-1}$  (Spitzer 1978), and  $n_e$  is the electron density. Equa-

tion (13) shows that ionization equilibrium is only possible if the density profile  $n_e \sim r^{-\gamma}$  has a slope less steep than  $\gamma = 3/2$  (Franco et al. 1990). Since the densities of the accretion solution (Fig. 2) are always less than the free-fall profile,  $\gamma = 3/2$ , this condition is always satisfied.

If the H II region is expanding, the speed of the ionization front at radius  $r_f$  is set by the balance of ionizing photons reaching the front  $J_f$ , and the number of atoms  $n_{\text{H}}$  crossing the front. Thus,

$$v_f = J_f / 4\pi r_f^2 n_{\text{H}}, \quad (14)$$

where

$$J_f = J_* - N_{\text{rec}},$$

and the number of recombinations,  $N_{\text{rec}}$ , is given by the integral in equation (13).

The velocity,  $v_f$ , of the ionization front determines whether a shock precedes the ionization front. The jump conditions (eqs. [9] and [10]) may be combined,

$$\frac{y_1}{y_2} = \frac{z_2}{z_1} = \frac{1}{2(K_1/K_2)^2} \times \{ (1 + y_1^2) \pm [(1 + y_1^2)^2 - 4y_1^2 K_1/K_2]^{1/2} \}. \quad (15)$$

The square root in equation (15) has real values only if the velocity of the gas relative to the front is greater or less than the critical values,

$$y_1 \geq y_{\text{R}} = (K_2/K_1)^{1/2} + (K_2/K_1 - 1)^{1/2}, \quad (16)$$

$$y_1 \leq y_{\text{D}} = (K_2/K_1)^{1/2} - (K_2/K_1 - 1)^{1/2}. \quad (17)$$

The subscripts “R” and “D” refer to the usual names R-type and D-type for fronts satisfying these conditions (Spitzer 1978; Dyson & Williams 1980; Shu 1992). If  $y_{\text{R}} > y_1 > y_{\text{D}}$  there is no solution of the combined jump conditions, and a shock front must precede the ionization front to compress and slow the incoming gas. Since  $y_{\text{R}} \sim 2(K_1/K_2)^{1/2}$ , which is twice the sound speed of the ionized gas, R-type fronts occur when the relative motion of the front and the gas is fast enough that a shock wave can not propagate ahead of the front. Conversely,  $y_{\text{D}} \sim (K_2/K_1)^{1/2}/2$ , and in this case, the front is moving below the sound speed of neutral gas, and again, no shock is propagated.

### 3. METHOD OF SOLUTION

Under the assumption of constant flow, the H II region is assumed to expand slowly relative to the dynamical time-scale of the ionized flow within the H II region. The velocities and densities of the ionized flow within the H II region are thus assumed to constantly adjust to the boundary conditions set at the ionization front which themselves are smoothly varying as the ionization front moves outward. The solution of the model consists in determining self-consistent values for the velocities and densities of the ionized and neutral flows, and the velocities of the ionization and shock fronts given the five parameters of the model—the stellar mass and ionizing flux, the two sound speeds, and the gas density at infinity. In terms of the mathematical solution, the position of the H II region boundary is treated as an additional parameter of the model.

It is possible that depending on the model parameters, there may be no self-consistent solution. For example, for a given density, the ionizing flux may be insufficient to achieve equilibrium with the rate of infall of neutral atoms or molecules and an H II region may not form at all. A nonexistent H II region in this condition is sometimes referred to as “quenched” (Yorke 1984; Walmsley 1995).

If the model parameters are such that a self-consistent solution is found with a stationary ionization front within the R-critical radius, the H II region would not evolve unless one of the five model parameters such as the ionizing flux were to change.

If the model parameters are such that the boundary of the H II region is beyond the R-critical radius, then the H II region will evolve hydrodynamically in pressure-driven expansion. The evolution is indicated mathematically by the existence of self-consistent solutions for any position of the H II boundary (for the same model parameters) all of which have outward velocities for the ionization and shock fronts. The evolution of the H II region then follows by assuming that the H II region transitions from one boundary position to the next at the velocity found for the ionization front at each boundary position.

The following two sections explain the method of solution in more detail. The method differs inside and outside of the R-critical point because of the absence or presence of a shock front preceding the ionization front.

### 3.1. Solution within the R-critical Radius

If the velocity of the infalling neutral gas relative to the ionization front is greater than the R-critical velocity (eq. [17]), then there is no shock preceding the ionization front. Since the velocity is supersonic with respect to the ionized gas, the front must be inside the sonic point,  $x_{c2} = K_1/2K_2$  of the ionized flow. Since the solution does not pass through the sonic point, the mass inflow rate within the H II region is not constrained by the sonic point, but instead will match the mass inflow rate in the neutral flow. The velocity and density profiles within the H II region (eq. [11]) can be determined by evaluating the constant  $\beta$  (eq. [12]) with  $\lambda_2 = \lambda_1$  and with  $y_{2f}$  and  $z_{2f}$  set by the jump conditions (eq. [9] and [10]) using the values for  $y_{1f}$  and  $z_{1f}$  established by the neutral accretion flow (eq. [2]), and the velocity of the ionization front (eq. [14]). The solution for the ionized flow then follows an inner portion of one of the streamlines that lies entirely above the sonic point (Fig. 1). Since the velocity of the ionization front itself depends on  $z_2$  through the equations of photoionization equilibrium (eqs. [13] and [14]), a self-consistent solution can be found iteratively.

Figures 3 and 4 show the neutral and ionized velocities and densities for the case of an H II region with  $K_1 = 100R$ ,  $K_2 = 20,000R$ ,  $N_{UV} = 1.89 \times 10^{49} \text{ s}^{-1}$ ,  $M = 40 M_\odot$ ,  $n_\infty = 1000 \text{ cm}^{-3}$ , and  $r_{ion} = 0.9r_c$ . The ionization front in this solution is stationary, and the H II region is therefore not evolving hydrodynamically.

### 3.2. Solution beyond the R-critical Radius

If the velocity of the infalling gas relative to the ionization front is below the R-critical velocity, then a shock front must precede the ionization front. Following the method of solution in the classic model without gravity, the velocity of the shock front can be determined once the velocity of the gas inside the ionization front is known. Where the classic

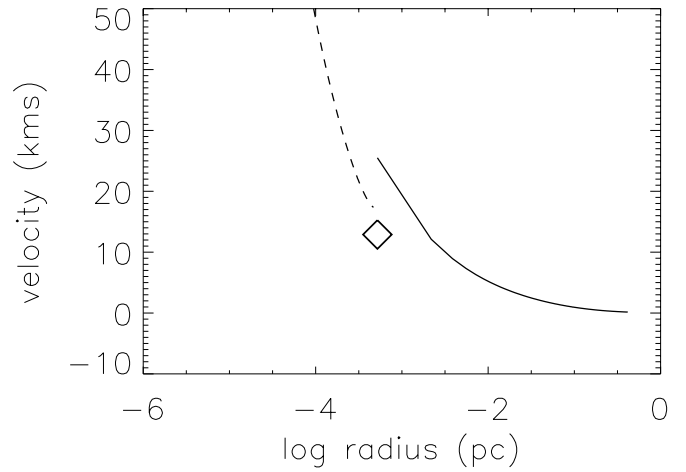


FIG. 3.—Velocities in the neutral (solid line) and ionized (dashed line) gases for a case described in text where the radius of ionization equilibrium is inside the R-critical point, which itself is just inside the sonic point of the ionized flow (diamond). The H II region boundary in this case consists of a stationary R-type ionization front with no accompanying shock.

model for pressure-driven expansion without gravity uses an assumption of constant density and the conservation equation to determine the velocity of the ionized gas, the model with gravity uses the assumption of constant flow within the accretion solution of the ionized gas to determine the ionized gas velocities. Knowing the velocity of the ionized gas,  $y_{2f}$ , just inside the ionization boundary, and the velocity of the ionization front,  $y_{ion}$ , the jump conditions (eqs. [9] and [10]) can be used to determine the velocity,  $y_{1f}$ , of the neutral gas just ahead of the ionization front. The notation is as follows:

$$\begin{array}{ccccccc}
 & & \rightarrow & & \rightarrow & & \\
 & & y_{ion} & & y_{shock} & & \\
 \leftarrow & | & \leftarrow & \leftarrow & | & \leftarrow & \\
 y_{2f} & & y_{1f} & y_{1s} & & y_{0s} & 
 \end{array} \quad (18)$$

Assuming that there are no velocity or density gradients in the postshock layer—the postshock layer is thin—then the gas velocity ahead of the ionization front,  $y_{1f}$ , is the same as

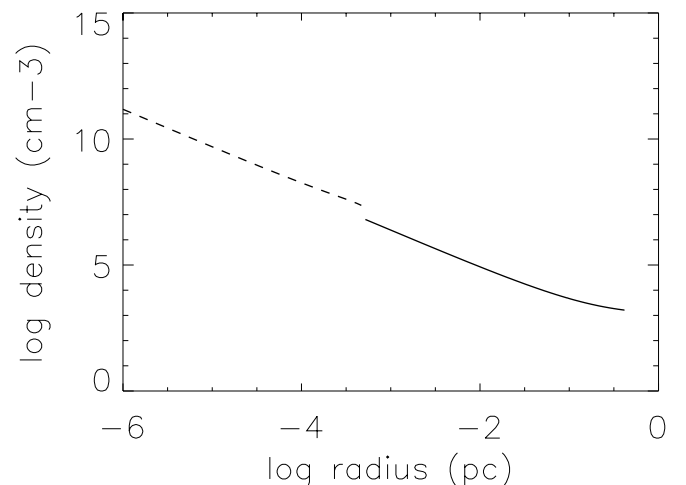


FIG. 4.—Same as Fig. 3, but plotting density instead of velocity

the gas velocity,  $y_{1s}$ , just behind the shock front. Now the velocity of the shock front can be found from the jump conditions knowing the gas velocities behind,  $y_{1s}$ , and ahead,  $y_{0s}$ , of the shock front. The gas velocity  $y_{0s}$ , ahead of the shock front is given by the velocity of the neutral accretion flow that is assumed to remain constant over time. Once the velocities of the fronts are known, the densities of the post-shock layer and the ionized gas behind the ionization front can be found from the jump conditions, calculating now in the reverse order starting with the known density of the neutral accretion flow. Since the speed of the ionization front also depends on the density of the ionized gas, a self-consistent solution can be found by iteration.

The velocity of the ionized gas,  $y_{2f}$ , just inside the ionization front is found in one of two ways depending on whether the ionization front is beyond or inside the sonic point,  $x_{c2}$ , of the ionized gas.

If the ionization front is beyond the sonic point, then the ionized flow must pass through the sonic point, and the velocity profile is fixed by the mass of the star, and the sound speed of the ionized gas. The velocity  $(K_1/K_2)^{1/2}$  at the sonic point,  $x_{c2} = K_1/2K_2$ , fixes the value of the constant  $\beta$  in equation (11), and this equation can be used to determine the ionized gas velocity at the position,  $x$ , of the ionization front.

If the ionization front is within the small range between the sonic point,  $x_{c2}$ , and the R-critical point where the shock front first separates from the ionization front when  $v_1 \sim 2c_2$ , the velocity of the ionized flow is not set by the sonic point. But over this range, the velocity of the gas leaving the ionization front may be assumed to be at its sound speed. The reason is that at the beginning of the range, at the R-critical point where the shock first separates, the velocity,  $y_{2f}$ , of the ionized gas behind the front will be at exactly the sound speed according to equations (16) and (17). At the end of the range, at the sonic point,  $x_{c2}$ , the velocity,  $y_{2f}$ , is also exactly at the sound speed. The range itself is small: if  $K_1 = 100R$  and  $K_2 = 20,000R$ ,  $N_{UV} = 2.01 \times 10^{49} \text{ s}^{-1}$  and  $M = 40 M_\odot$ , then  $x_{c2} = 0.0025$  and  $x_{Rcrit} = 0.00245$ , and it is reasonable to assume that the gas velocity maintains the same value within this range as at the end points. Because the R-critical front is hydro-

dynamically equivalent to a combination of a D-critical front plus a preceding isothermal shock moving at the same velocity, and because the gas velocity just behind a D-critical front is also the sound speed, then it is reasonable to assume that the ionization front remains at a D-critical state over this range. While the velocity of the ionized gas leaving the ionization front remains constant at the sound speed over this range, the velocity of the shock is only equal to velocity of the ionization front exactly at the R-critical point. After the R-critical point, the velocity of the shock front will always be a little faster than the velocity of the ionization front because the speed of the infalling neutral gas will always be less at any larger radii. Thus, the shock front will separate from the ionization front at the R-critical point and move ahead thereafter. Its velocity at any radius between the R-critical point and sonic point,  $x_{c2}$ , may be determined by the same method as described in § 3, starting from  $y_{2f}$  and working forward to the shock velocity.

#### 4. THE COURSE OF THE EVOLUTION

##### 4.1. Ionization Boundary within the R-critical Radius

If the star at the center of the H II region has an ionizing flux such that a stationary radius of ionization equilibrium is within the R-critical radius, then the H II region cannot expand by thermal pressure. At these small radii, the infall velocities are everywhere above the sound speed of the ionized gas, the gravitational attraction of the star dominates over the thermal pressure, and once ionization equilibrium is achieved, the H II region can only expand by an increase in the flux of ionizing photons. The continuing accretion provides a natural mechanism whereby additional stars may form or existing stars may increase their luminosities by gaining mass. However, the physics of these processes are not addressed by the simple model described in this paper.

Table 1 lists for several values of the gas density at infinity, the ionizing flux and the approximate spectral type and mass required to form an initial H II region at  $10 R_\odot$ . The table then lists the ionizing flux and approximate spectral type required to maintain an H II region trapped at the R-critical radius. Since the densities in Table 1 are quite

TABLE 1  
TRAPPING THE H II REGION

$n_\infty$ ( $\text{cm}^{-3}$ )	INITIATED AT $10 R_\odot$			TRAPPED AT R-CRITICAL			INFALL RATE ( $M_\odot \text{ yr}^{-1}$ )
	$\log(N_*)^a$ ( $\text{s}^{-1}$ )	Type	Mass ( $M_\odot$ )	$\log(N_*)^a$ ( $\text{s}^{-1}$ )	Type	Mass ( $M_\odot$ )	
10.....	43	B4	6	45	B1	13	$2 \times 10^{-8}$
100.....	44	B3	8	47	B0	18	$5 \times 10^{-7}$
1000.....	45	B1	13	49	O5.5	38	$1 \times 10^{-5}$
10000.....	46	B0.5	16	51	Cluster	>1500	$6 \times 10^{-3}$

NOTES.—Given a density at infinity in the first column, the table shows the ionizing flux and approximate stellar type that would create an H II region trapped at a radius of  $10 R_\odot$  and also for a radius of R-critical. The difference between the approximate stellar masses for the types associated with the two radii indicate the amount of mass that would have to be gained by a single star to increase its rate of ionizing photons to expand the H II region from  $10 R_\odot$  to R-critical. The infall rates give an indication of the time required to accrete this much mass. Infall rates refer to the initial lower masses of the stars. The ionizing flux of  $10^{51} \text{ s}^{-1}$  requires a cluster of stars, for example 24 stars of type O4 for a minimum total stellar mass of  $1500 M_\odot$  or more stars of a later type.

<sup>a</sup> Panagia 1973.

modest compared to those normally inferred for massive star forming regions, trapping of an H II region with a boundary between the stellar radius and the R-critical radius is certainly possible for a range of spectral types. If, as speculated, the H II region is to grow through the increase in the ionizing flux of the stars powering it, then the evolutionary timescale of the H II region in the trapped phase must be on the order of the accretion timescale, or quite slow compared to the dynamical timescale of the H II region.

4.2. Ionization Boundary beyond the R-critical Radius

Once the H II region boundary is beyond the R-critical point, then it will expand by thermal pressure whether or not the ionizing flux continues to increase. This can be determined by noting that when the ionization boundary is at any radius beyond the R-critical radius, the velocity of the ionization and shock fronts found from the self-consistent solution is always non zero and outward with respect to the star, implying continuing expansion.

Figure 5 shows the velocities for the case where  $K_1 = 100$ ,  $K_2 = 20,000$ ,  $N_{UV} = 2.01 \times 10^{49} \text{ s}^{-1}$ ,  $M = 40 M_{\odot}$ , and the number density at infinity,  $n_{\infty} = 1000 \text{ cm}^{-3}$ . The solution shows that as the H II region expands, the velocity of the front increases to a maximum, the increase coming about because of the decreasing infall speed of the neutral gas at larger radii. The subsequent decrease in the velocity of the ionization front is due to the reduced pressure difference across the H II region boundary as the ionized gas becomes rarefied because of the reduced mass infall rate across the H II region boundary. At large radii, where the ionization front speed has slowed almost to zero, the velocities of the shock and ionization fronts begin to differ significantly, and the shock will move far ahead of the ionization front.

Figure 6 shows the densities of the post-ion front ionized gas, and the postshock and preshock neutral gases as a func-

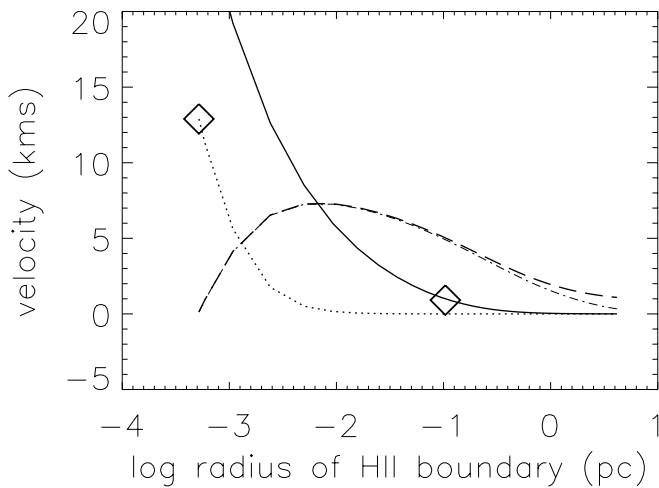


FIG. 5.—Inward velocities of the ionized (dotted line) and neutral (solid line) flows and the outward velocities of the shock (dashed line) and ionization (dash-dotted line) fronts as a function of the radius of the H II region boundary. At any radius, imagine a vertical line drawn down the graph. The velocities of the gas and fronts at this radius are found from the intersections of the curves with the vertical line. The velocity of the ionized gas is the velocity just behind the ionization front, while the velocity of the neutral gas is the velocity just before the shock front. Because of the restriction imposed by eq. (2), these gas velocities are also the velocities along a streamline of the accretion flow. The sonic points,  $r_{c2}$  and  $r_{c1}$  are marked as diamonds. The front velocities have been multiplied by  $-1$ .

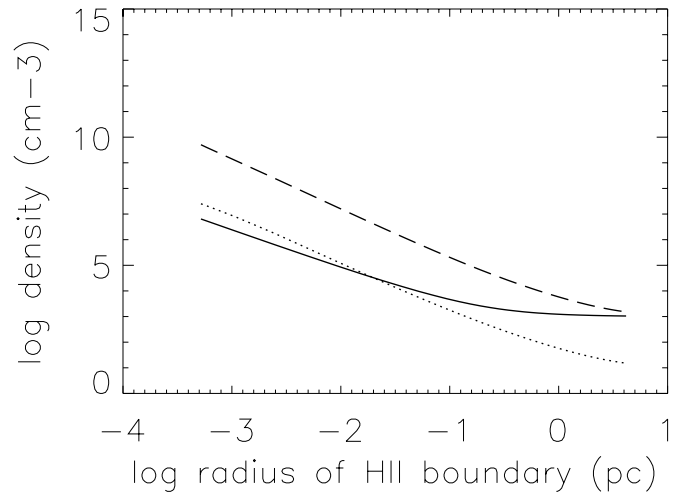


FIG. 6.—Densities of the preshock neutral gas (solid line), postshock neutral gas (dashed line), and post-ion front ionized gas (dotted line) as a function of the radius of the H II region boundary. For any radius, the densities are read from the intersection of a vertical line at this radius with the curves. The density of the neutral flow is also the density along a streamline of the neutral accretion flow, but this equivalence does not hold for the other two densities.

tion of the position of the ionization front (x-axis). As the ionization front moves out to larger radii, the postshock compression is steadily reduced as the shock velocity decreases because of the decrease in the infall speed of the neutral material. However, the reduction in density across the ionization front, necessary to maintain pressure balance between the hot ionized gas and the cold neutral gas, remains nearly constant as a function of the ionization front position. These two effects combine to yield a continuously decreasing mass infall rate across the H II region boundary. Figure 7 shows this decrease in the mass infall rate through

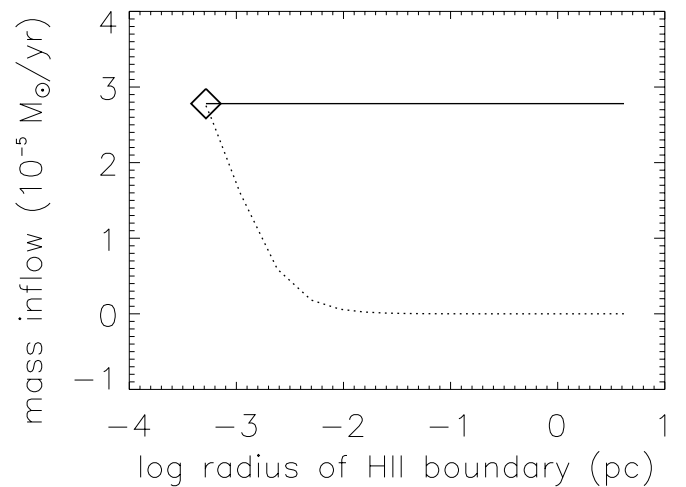


FIG. 7.—Mass infall rate as a function of the radius of the H II region boundary in the neutral flow (solid line) and ionized flow (dashed line). The accretion rate in the neutral flow remains constant over time. The accretion rate in the ionized flow is equal to the rate in the neutral flow at radii less than the R-critical radius (diamond) but decreases rapidly thereafter. The excess matter piles up between the ionization and shock fronts.

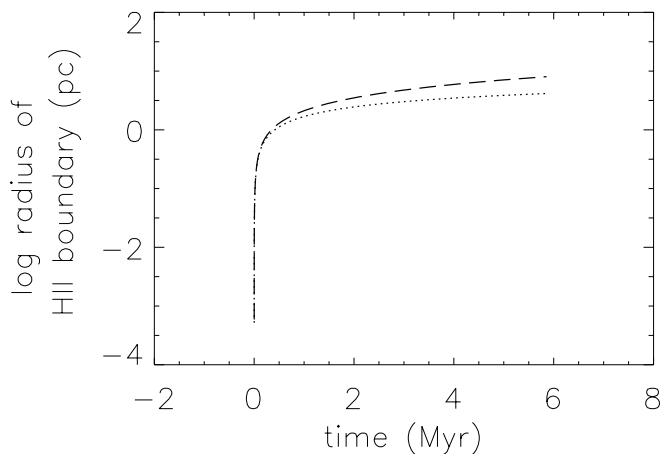


FIG. 8.—Position of the ionization (*dotted line*) and shock (*dashed line*) fronts as a function of time past the time when the H II region boundary first reaches the R-critical radius. Below the R-critical radius, the H II region does not evolve hydrodynamically. After the R-critical radius, the H II region enters a phase of rapid expansion that gradually decreases in rate. The separation of the shock and ionization fronts increases continuously over time.

the H II region as a function of the position of the ionization front. Also plotted is the infall rate in the neutral zone, which is a constant because the accretion flow in the neutral gas outside of the boundary around the H II region remains unaware of the expanding H II region. The excess matter accumulates at the H II region boundary in the dense post-shock layer, a characteristic shared with the classic model without gravity.

Figure 8 shows the timescale for the evolution beyond the sonic point,  $x_{c2}$ . The expansion is initially very rapid but slows as the expansion progresses. The shock front position is the only quantity calculated in this model which must be found by integrating the model over time (or radius). The timescale of the model in the expansion phase is similar to that in the classic model without gravity because the ionization front velocities in both models are of the order of the ionized sound speed. However, with gravity, the expansion phase begins only when the radius of ionization equilibrium is greater than the R-critical radius. As discussed in § 4.1, smaller H II regions do not evolve hydrodynamically, and the timescale for the radius of ionization equilibrium to reach the R-critical radius and begin hydrodynamic expansion must be set by the timescale required to increase the ionizing flux through stellar evolution or through an increase in the mass or number of the stars due to accretion.

## 5. IMPLICATIONS FOR THE EVOLUTIONARY STAGES OF A HIGH-MASS STAR-FORMING MOLECULAR CORE

The model for pressure-driven expansion describes the interaction of the ionization and shock fronts of an expanding H II region and the infalling gas of an idealized accretion flow. The model is not an adequate description for the evolution of a star-forming molecular core because it does not include many important physical processes such as rotation, magnetic fields, stellar winds, and stellar evolution. Nevertheless, the evolution of the pressure-driven expansion model with gravity implies a somewhat different scenario for the evolution of a high-mass star-forming molecular core than is implied by the expansion model without gravity.

1. Since accretion does not end as soon as an H II region is formed, a young high-mass star may begin nuclear burning and evolve to earlier spectral types as it gains mass. If so, the ionizing flux of the star will increase slowly over time, in contrast to the model without gravity in which the radiation from the star is assumed to turn on suddenly and remain constant thereafter. Because the increase in ionizing flux is tied to the accretion rate, the timescale for accretion through the H II region will be relatively long—on the order of the free-fall timescale of the molecular core.

2. Once the ionizing flux is sufficient to maintain an H II region larger than the R-critical radius, a number of events happen in short order. The H II region begins to expand dynamically, and the velocity of the boundary increases rapidly to the order of the sound speed of the ionized gas. The expansion effectively terminates the accretion through the H II region. At this point, a stellar wind that would have been inhibited by the mass infall as long as  $\dot{M}_{\text{acc}} > \dot{M}_{\text{wind}}$  may develop, although the details of this would depend on the mode of accretion—spherical or disklike—near the star. The H II region itself will rapidly expand to a size on the order of  $(T_{\text{ionized}}/T_{\text{molecular}})^{1/3}$  larger than its R-critical size as it achieves approximate pressure equilibrium with the surrounding cold neutral gas. The timescale for this phase of hydrodynamic expansion is very short compared with the preceding and following evolutionary stages.

3. Finally, the H II region then enters a relatively long period of subsonic expansion that will be terminated by a massive stellar wind or supernova as one or more stars in the H II region reaches the end of its main-sequence lifetime. This phase of slow expansion could last longer than the typical  $10^6$  yr lifetime of a massive O star if the H II region is powered by a small group of later type O stars or early B stars rather than a single star of very high mass.

## REFERENCES

- Bondi, M. 1952, *MNRAS*, 112, 195  
 Dyson, J., & Williams, D. 1980, *The Physics of the Interstellar Medium* (New York: Wiley)  
 Franco, J., Tenorio-Tagle, G., & Bodenheimer, P. 1990, *ApJ*, 349, 126  
 Garay, G., & Lizano, S. 1999, *PASP*, 111, 1049  
 Keto, E. 2002, *ApJ*, 568, 754  
 Mathews, W., & O'Dell, C. 1969, *ARA&A*, 7, 67  
 Mestel, L. 1954, *MNRAS*, 114, 437  
 Panagia, N. 1973, *AJ*, 78, 929  
 Parker, E. 1958, *ApJ*, 128, 664  
 Shu, F. 1992, *The Physics of Astrophysics, Vol. II, Gas Dynamics* (Mill Valley: University Science Books)  
 Spitzer, L., Jr. 1978, *Physical Processes in the Interstellar Medium* (New York: Wiley)  
 Walmsley, M. 1995, in *Rev. Mexicana Astron. Astrofis. Ser. Conf. 1, Circumstellar Disks, Outflows, and Star Formation*, ed. S. Lizano & J. M. Torrelles (Mexico, DF: Inst. Astron., UNAM), 137  
 Yorke, H. 1984, *Workshop on Star Formation*, ed. R. D. Wolstencroft (Edinburgh: Publ. R. Obs. Edinburgh), 63  
 ———. 1986, *ARA&A*, 24, 49